Veterinary Immunology and Immunopathology 214 (2019) 109891

Contents lists available at ScienceDirect

Veterinary Immunology and Immunopathology

journal homepage: www.elsevier.com/locate/vetimm

Research paper

Tumor microenvironment and stroma in intestinal adenocarcinomas and associated metastases in Atlantic salmon broodfish (*Salmo salar*)

Håvard Bjørgen[a], Hege Hellberg[b], Oskar Mongstad Løken[a], Gjermund Gunnes[a], Erling Olaf Koppang[a], Ole Bendik Dale[c,*]

[a] Faculty of Veterinary Medicine, Norwegian University of Life Sciences, Oslo, Norway
[b] Fish Vet Group Norge, Oslo, Norway
[c] Norwegian Veterinary Institute, Oslo, Norway

ARTICLE INFO

Keywords:
Adenocarcinoma
B cell
Inflammation
Major histocompatibility complex
Mast cell
Stroma
T cell
Teleost
Tumor microenvironment

ABSTRACT

Animal models are invaluable tools in cancer research. In this context, salmon is a promising candidate. Intestinal adenocarcinoma with metastases may be induced as a consequence of a plant-based diet triggering the inflammation – dysplasia- carcinogenesis pathway. Here, we investigate the stroma and the presence and nature of immune cells in such tumors by staining for mast cells, immunohistochemistry for T cells and antigen-presenting cells and *in situ* hybridization for B cells. In intestinal tumors, substantial amounts of T cells were detected in the stroma, whilst MHC class II$^+$ cells were mainly among the cancerous cells. Ig$^+$ cells were observed primarily in the tumor periphery. Mast cells showed a strong association with stroma. In metastases, scarce amounts of T cells were detected, whilst MHC I and II-reactivity varied, some tumors being completely negative. Ig$^+$ cells were scattered around the metastatic tissue in no particular pattern, but were occasionally observed within clusters of tumor cells. Small numbers of mast cells were detected in the stroma. To the best of our knowledge, this is the first report addressing immune cells in fish tumors. The teleost tumor microenvironment seems comparable to that of mammals, making fish interesting model animals in oncoimmunology research.

1. Introduction

Animal models are valuable tools for studying the pathogenesis of human cancers. The mouse has been the traditional model animal, however, other organisms such as zebrafish (*Danio rerio*) also play increasingly important roles in cancer research (Yee et al., 2015). Studies addressing tumor immunology in higher vertebrates have shown that the impact of the immune system within the tumor microenvironment is of great importance in cancer development (Giraldo et al., 2019). The close conservation between human and zebrafish tumor-generating mechanisms at molecular, cellular and tissue levels (Etchin et al., 2011; Liu and Leach, 2011) argues that the species might share common anti-tumor responses. Still, there are limited studies addressing the tumor microenvironment in teleost fish and possible comparative features are unknown. To the best of our knowledge, no reports have so far reported on the content of different immune cells in fish tumors. Hence, investigations in this field of research are warranted.

Although malignant neoplasms are rarely reported in fish compared with mammals (Vergneau-Grosset et al., 2017), intestinal adenocarcinomas with metastasis have been described in Atlantic salmon (*Salmo salar*) broodfish (mature fish used in aquaculture for breeding purposes) in association with chronic, feed-induced inflammation (Dale et al., 2009). The pathogenesis appears similar to that of inflammatory bowel disease (IBD)-tumorigenesis in humans following the enteritis – dysplasia – tumorigenesis pathway. Early stages of carcinogenesis have also been reported in younger production fish in association with inflammation (Bjørgen et al., 2018). In contrast to salmon, naturally occurring (i.e. not intentionally induced) intestinal adenocarcinomas in zebrafish showing an inflammation-dysplasia-carcinogenesis pathway are independent of diet and seem to have an infectious etiology (Burns et al., 2018; Paquette et al., 2013). The recurrent observations of pathological changes in salmonid intestine including inflammation, dysplasia, ectopic epithelial cells and tumor islands argue that farmed salmon are prone to such gastrointestinal changes. Furthermore, the seemingly high ability for metastasis of these cells, and the subsequent forming of secondary tumors in other organs makes the salmon an appealing model for oncology research.

The morphology and key immune parameters of the gastrointestinal

* Corresponding author at: Section of Aquatic Biosecurity, Norwegian Veterinary Institute, Ullevålsveien 68, Post box 750 Sentrum, 0106, Oslo, Norway.
E-mail addresses: havard.bjorgen@nmbu.no (H. Bjørgen), hege.hellberg@fishvetgroup.com (H. Hellberg), oskar.fiskadal.loken@nmbu.no (O.M. Løken), gjermund.gunnes@nmbu.no (G. Gunnes), erling.o.koppang@nmbu.no (E.O. Koppang), ole.b.dale@vetinst.no (O.B. Dale).

https://doi.org/10.1016/j.vetimm.2019.109891
Received 8 March 2019; Received in revised form 26 June 2019; Accepted 3 July 2019

tract in wild-caught salmon was recently described, showing the presence and localization of key immune cells (T cells and MHC class II$^+$ cells) (Løkka et al., 2013, 2014). MHC class II$^+$ cells or antigen-presenting cells are presumed to be mostly macrophage-like cells, as a specific macrophage marker is not available for fish cells. Here, we wanted to evaluate the host immune reaction and describe the tumor microenvironment and stroma in intestinal adenocarcinomas related to the use of plant ingredients in feed to the strictly carnivorous salmon. More specifically, we aimed to investigate the presence and distribution of macrophage-like cells, T cells and B cells in both primary intestinal tumors and in hepatic, heart and kidney metastases. In addition, the involvement of eosinophilic granular cells, which are normally present in large numbers in the intestinal mucosa, was studied. Eosinophilic granular cells have an eccentrically placed, ovoid nucleus and a cytoplasm filled with granules, have a predominantly perivascular location and are considered analogous to mast cells in mammals (Hellberg et al., 2013; Reite and Evensen, 2006). In the present work, these cells will be referred to as mast cells.

We show that the tumors in Atlantic salmon indeed are rich in immune cells and that their nature and distribution are comparable with similar changes in mammals. The results reveal that many host immune responses to tumors are conserved in species separated by millions of years of evolution and thus are ancient in their nature. Hence, teleost fish seem well suited for future research in tumor immunology.

2. Materials and methods

The material used in this investigation has been described in detail previously (Dale et al., 2009). Briefly, groups of commercially reared Atlantic salmon having been fed a plant-based diet developed intestinal adenocarcinoma with a frequency up to 29% in the most affected groups of fish. Here, liver metastases were observed with a frequency up to 11.35%. In addition, a feed experiment was conducted, demonstrating an association between the actual feed and intestinal carcinogenesis (Lyngstad et al., 2007).

Tissue samples from all groups were collected on formalin, routinely processed and paraffin-embedded (Dale et al., 2009). From this material, intestinal tumors (n = 50) and metastases (n = 50) were stained with hematoxylin and eosin (HE), Van Gieson's (VG) stain and periodic acid schiff (PAS) stain according to standard procedure (Bancroft and Gamble, 2008). Selection criteria for further analysis were defined as tumors appearing representative for the observed condition (content of cells conformal with the diagnosis adenocarcinoma; i.e. PAS-positive cells and with a tumor size varying from a few up to 25 mm in diameter). Such cells were previously shown to be cytokeratin positive by immunohistochemistry (IHC) (Dale et al., 2009).

2.1. Detection of immune cells

To address the presence of immune cell in primary tumors and metastases, a haphazard sub-selection of intestinal tumors (n = 7) and liver (n = 8), kidney (n = 4) and heart (n = 4) metastases were investigated by Martius-Scarlet-Blue (MSB) staining, IHC and *in situ* hybridization (ISH).

Sections were stained with MSB for identification of mast cells (Hellberg and Bjerkås, 2000). Immunohistochemical analysis with cell markers recognizing CD3, CD8, MHC class I and MHC class II was performed as described elsewhere (Bjørgen et al., 2018) (Table 1). Briefly, sections were de-paraffinated and autoclaved. Inhibition was done with phenylhydrazin and blocking with goat normal serum diluted in 5% bovine serum albumin/tris-buffered saline (BSA/TBS). Primary antibodies were diluted in 1% BSA/TBS and incubated for 30 min in room temperature. The sections were further incubated with an anti-mouse secondary antibody (Dako EnVision kit) and developed with DAB/AEC to evoke color (brown/red). Negative controls were performed without primary antibody.

Table 1
Primary antibodies used for immunohistochemical analysis.

Antibody/dilution	Reactive against
Sasa MHC class I F3-31, 1:100	Alpha 3 domain of MHC I alpha chain
Sasa MHC class II F1-12, 1:400	Beta 2 domain of MHC II beta chain
Anti-CD3, 1:400	Epsilon chain of the CD3 transmembrane protein
Sasa CD8 F1-29, 1:100	CD8α, a part of the CD8 complex

The entire sub-selection of intestinal tumors and metastases was subjected to ISH targeting immunoglobulin (IgM and IgT) RNA using RNAscope® 2.5 HD Assay - RED (Advanced Cell Diagnostics, Newark, CA) according to the manufacturer's instructions. To investigate IgM RNA expression, a custom 20ZZ RNAscope® probe was constructed, targeting bp 219–1157 of NCBI Reference Sequence XM_014203125.1. To investigate IgT RNA expression, an 18ZZ RNAscope® probe was constructed, targeting bp 3–883 of three slightly different functional IgT transcripts (Yasuike et al., 2010). Head-kidney from unaffected salmon was used as positive control for both probes (head-kidney of salmon is a B-cell-containing immune structure). RNAscope probe against the bacterial gene dapB (#701021) was used as negative controls in head-kidney and tumor sections to confirm absence of background and/or non-specific cross-reactivity of the assay.

3. Results

3.1. Peritumoral tissue morphology and stroma in intestinal tumors and their metastases

An inflamed mucosa and ectopic epithelial cells in the *lamina propria* were observed in the surrounding tissue of the primary intestinal tumors. A prominent and well-developed stroma was evident in all primary tumors of the intestine. Van Gieson's stain revealed abundant thick collagen fibers surrounding tumor islands (Fig. 1A). Similarly, the connective tissue stroma of most hepatic metastases was prominent (Fig. 1B) and even formed a connective tissue capsule in one individual, creating a distinct demarcation from the liver parenchyma. Investigated heart metastases did not show any supporting stroma (Fig. 1C), whilst only one of the kidney metastases had a distinct stroma (Fig. 1D).

3.2. Immune cells in primary intestinal tumors

In the tumor environment, inflammatory cells were identified in all samples. Mast cells were mainly observed associated with connective tissue, diffusely interspersed in the fibrous stroma (Fig. 2A) and only a few were present in the tumor cell islands (Fig. 2B). Immunostaining for CD3, a pan T cell marker, showed immuno-positive cells mostly confined to the tumor stroma (Fig. 3A) and often assembled in cell-dense foci. In the following, CD3$^+$ cells will also be termed T cells. Single T cells were occasionally embedded among cancerous cells (Fig. 3B). Areas with numerous T cells were detected at the invasive front in four of the tumors (Fig. 3C) with few immuno-positive cells present towards the luminal side, in the depth of the tumor tissue.

Mast cells followed the pattern of T cells, being more numerous at the invasive front and less at the luminal front. Degranulation of mast cells seen as extracellular granula was mainly observed at the edges of tumors and in the inflamed submucosa. In the central areas of the tumors, degranulation of mast cells was less frequent.

Immunostaining for CD8 revealed sparse amounts of cytotoxic cells in the tumor tissue. Immuno-positive cells were scattered in the tissue (Fig. 3D), mostly located within islands of cancerous cells. Single immuno-positive cells were occasionally detected in the stroma.

MHC class I reactivity varied between cancerous cells within the same tumor (Fig. 3E). All cancerous cells towards the epithelium and

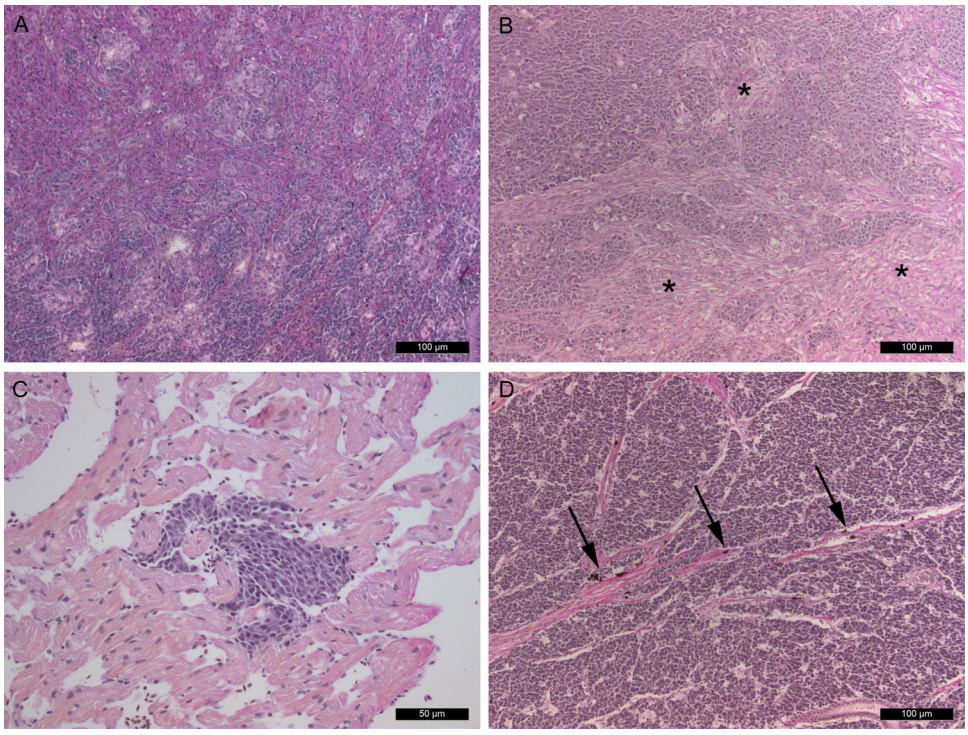

Fig. 1. Stroma of primary intestinal tumor and metastases. Van Gieson's staining. A) An intestinal tumor with a highly developed stroma between cancerous cell islands. B) A hepatic metastasis with distinct and pronounced stroma (asterisks). C) A heart metastasis in the spongious layer of the ventricle without any supporting stroma. D) A kidney metastasis with multiple collagenous bands throughout the cancerous tissue. Note the presence of melano-macrophages in the stroma (arrows).

lamina propria were intensely immuno-positive (at the tumor-host interface) (Fig. 3F), however, weakly stained cancerous cells and areas without detectable immuno-reactivity were seen peripherally in the tumors towards the lumen of the intestine. Additionally, distinct immuno-reactivity was observed in single cells in some tumor cell clusters (Fig. 3G). These cells were easily distinguishable from the surrounding cancer cells. Staining was also detected in the seemingly unaffected epithelium of the intestinal folds. The stroma was generally MHC class I negative, but occasional immuno-positive single cells were present.

MHC class II$^+$ cells infiltrated the cancer cell islands (Fig. 3H). Dense foci with multiple immuno-positive cells were evident in close proximity to the *lamina propria* (Fig. 3I), but were occasionally detected elsewhere in the tumor.

ISH targeting IgM transcripts revealed abundant positively stained cells (hereafter IgM$^+$ cells) accumulated in the stroma in the edges of the tumors towards the intestinal folds (Fig. 4A). Vast amounts of positive cells could also be detected in the *lamina propria* under intact folds. Cells positive for IgT transcripts (hereafter IgT$^+$ cells) showed a similar distribution as IgM$^+$ cells, though their numbers were generally fewer (Fig. 4B).

3.3. Immune cells in hepatic metastases

Scattered CD3$^+$ cells were consistently detected in the unaffected liver tissue. However, only a few T cells were present in the hepatic tumors. Scarce CD3$^+$ cells were scattered throughout the metastatic tissue, mostly located among the cancerous cells (Fig. 5A and B).

CD8$^+$ cells were detected in sparse amounts in one liver metastasis (Fig. 5C). These cells were confined to one focal area in the tumor tissue.

Immuno-staining for MHC class I revealed great diversity among different liver metastases. Four of the metastases showed no reaction, two showed a varying reaction with both positive and negative cancerous cells (Fig. 5D), whilst two were strongly positive. Of these two individuals, one displayed a deviating phenotype with massive immuno-positive dendritic-like cells throughout the tumor tissue (Fig. 5E).

Few and scattered MHC class II$^+$ cells were detected in four of the metastases. These cells were generally seen among the cancerous cells. Occasional foci with multiple immuno-positive cells were observed in two individuals (Fig. 5F). Few mast cells were observed in the hepatic tumors, and those present were mainly found in the stromal connective tissue.

In situ hybridization studies revealed IgM$^+$ cells adjacent to and in vessels in the liver parenchyma, with some positive cells in the border

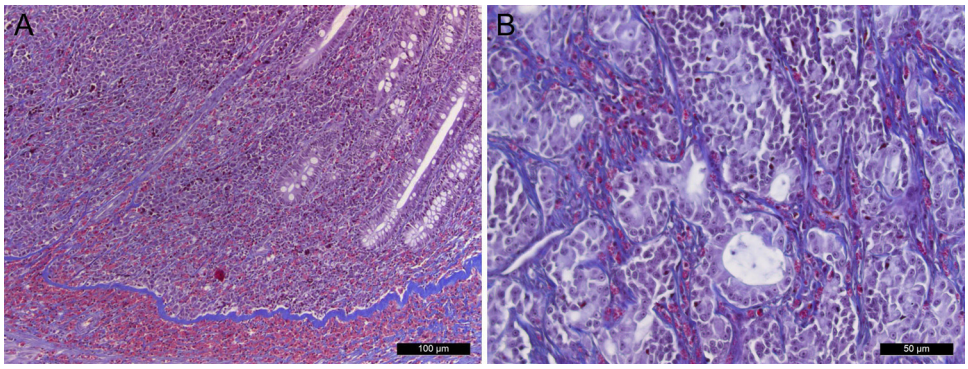

Fig. 2. Localization of mast cells in intestinal tumor. MSB staining. A) Mast cells (red) are present in the connective tissue in large numbers on both side of the collagenous band; *stratum compactum* (blue). B) Intestinal tumor cancerous cell islands with few or no mast cells among the cancer cells. The mast cells (red) are mainly confined to the stroma (blue).

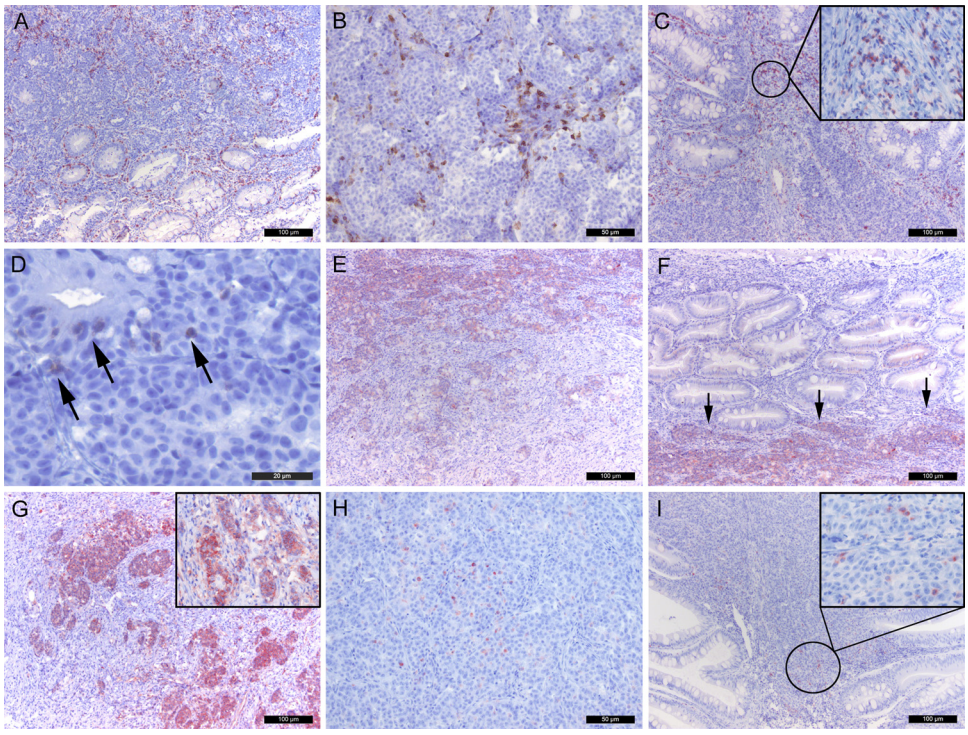

Fig. 3. Immune cells in primary intestinal tumors (IHC). A) Substantial amounts of $CD3^+$ cells (brown) are seen in the tumor tissue. Most cells are located peritumorally in the stroma. B) Higher magnification of cancer islands, with occasional $CD3^+$ cells (brown). C) Invasive front of tumor, showing high densities of $CD3^+$ cells (red). High magnification image shows multiple $CD3^+$ cells among cancerous cells. D) Cancer island showing sparse amounts of $CD8^+$ cells among cancerous cells (arrows). E) Low magnification of tumor showing varied MHC class I staining (red) in tumor tissue. F) MHC class I staining showing high density of MHC class I^+ cells (red) at the tumor-host interface (arrows) in close proximity to the base of the intestinal folds (cross section) and weak or no staining in the *lamina propria* and in the intestinal epithelium. G) MHC class I staining of tumor tissue. The amount of MHC class I^+ cells (red) varies between tumor cell clusters. High magnification image shows immuno-positive cancer cell clusters and less intensely stained cells in the stroma. H) MHC class II staining of tumor tissue. MHC class II^+ cells (red) are mainly present in cancer island. I) Foci of MHC class II^+ cells (red) at tumor-host interface, close to the *lamina propria*. High magnification image shows scattered MHC class II^+ cells among cancer cell cluster.

between seemingly unaffected liver tissue and cancerous cells (Fig. 6A). This demarcation was especially evident in the liver tumor with an advanced connective tissue capsule. This tumor was almost devoid of IgT^+ cells. In an elaborate metastasis where the liver parenchyma was entirely displaced by cancerous tissue, multiple IgM^+ cells were detected among cancerous cells and in the stroma (Fig. 6B). Multiple IgT^+ cells were seen in the same tumors (Fig. 6C).

3.4. Immune cells in heart metastases

MHC class I and II staining were negative in all heart metastases. Some immuno-positive cells were seen in one individual as part of an inflammatory foci without any visible tumor cells. Single $CD3^+$ cells appeared scattered in all hearts investigated, with no obvious connection to any metastatic tissue. $CD8^+$ cells were not detected in any of the samples. Mast cells were not observed in the heart metastases.

IgM^+ cells were seen in all three layers of the heart and in both the spongious and compact layers of the ventricle. The vast majority of positive cells were seen in the epicardium, conformal with epicarditis. Positive cells appeared both in relation to metastases and in myocardium without cancerous cells (Fig. 6D). IgT^+ cells were less frequent and appeared scattered in the myocardium, occasionally in focal accumulations in relation to metastases

3.5. Immune cells in kidney metastases

$CD3^+$ cells appeared abundantly in all kidney tissues, and in relation to the metastases. However, no $CD8^+$ cells were detected in relation to tumor tissue. MHC class I^+ cells were detected in one individual only. In this metastasis, the reactivity varied between cancerous cell islands, from no staining at all to a very strong signal. Scattered MHC class II^+ cells were observed in the same metastasis, both in the stroma and among cancerous cells (Fig. 7A). Additionally, sparse melano-macrophages were present in the stroma. T cells and melano-macrophages were detected around a focal area of metastatic tissue, encircling a focus of metastatic cells (Fig. 7B). Intense MHC class I reactivity was registered within this organization of T cells (Fig. 7C). Adjacent tubular epithelium displayed varying MHC class I reactivity. Few mast cells were observed in the kidney metastases, and those present were mainly found in stromal connective tissue.

In situ hybridization revealed substantial amounts of IgM^+ cells throughout the kidney interstitium with an even distribution (Fig. 8A). IgT^+ cells were less frequent with similar distribution as the IgM^+ cells (Fig. 8B).

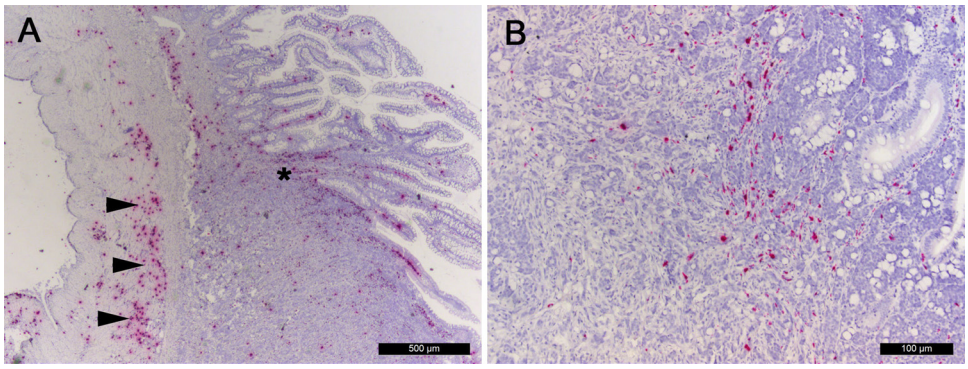

Fig. 4. ISH of primary tumors targeting IgM and IgT transcripts. A) Low magnification of intestine showing distribution of IgM^+ cells (red). Accumulations of IgM^+ cells are seen in tumor stroma (*), *lamina propria* and connective tissue in tunica muscularis (arrowheads). B) Higher magnification of intestinal mucosa, showing distribution of IgT^+ cells.

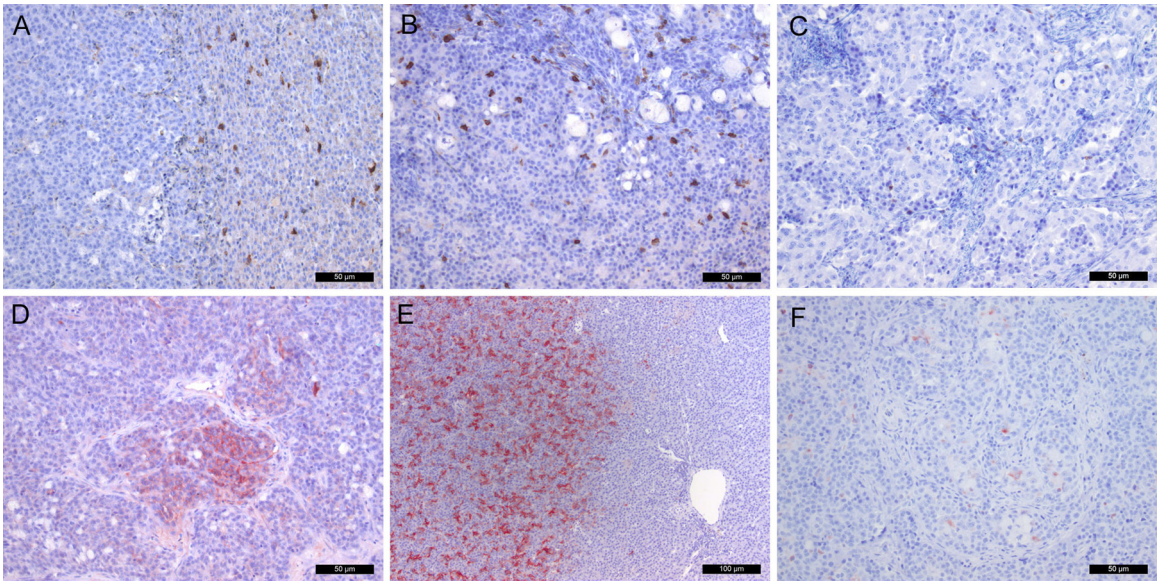

Fig. 5. Immune cells in hepatic metastases. A) CD3 staining of the tumor-host interface showing scattered $CD3^+$ cells (brown) in the metastatic tissue (right side of the image). B) $CD3^+$ cells (brown) distributed among cancer cells in the metastatic tissue. C) A focal infiltrate with few $CD8^+$ cells (brown) in the metastatic tissue. D) Focal distribution of MHC class I^+ cells (red) in the metastatic tissue. The surrounding cancer cells appear immuno-negative. E) Diffuse distribution of MHC class I^+ cells (red) throughout the metastatic tissue with a sharp demarcation to the unaffected liver tissue. The tumor shows a deviating phenotype with massive immuno-positive dendritic-like cells throughout the metastatic tissue F) MHC class II staining of metastatic tissue showing a foci of MHC class II^+ cells (red).

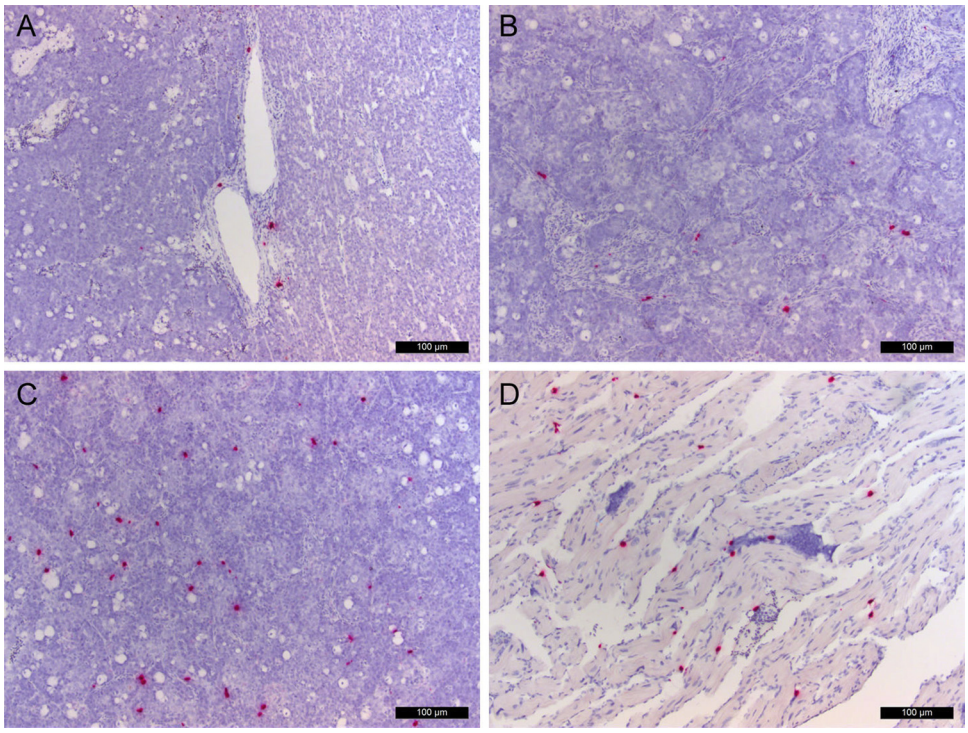

Fig. 6. ISH of hepatic and cardiac metastases targeting IgM and IgT transcripts. A) IgM staining of liver. IgM^+ cells (red) show a mainly perivascular location. B) IgM staining of tumor tissue in liver. IgM^+ cells (red) are seen in stroma and among cancerous cells. C) Ig T staining of same tumor as in B, showing a higher density of IgT^+ cells (red). D) Ig M staining of heart. IgM^+ cells (red) are scattered in myo- and endocardium and are also present in tumor tissue. Empty vacuoles represents mucus-containing cancer cells (A–C).

3.6. Controls

All negative controls in the IHC experiments were negative (data not shown). In the ISH experiments, control tissue from head-kidney confirmed the presence of IgM^+ and IgT^+ cells, conformal with the expected numbers and distribution (data not shown). Head-kidney and tumor tissue subjected to the negative control probe were negative (data not shown).

4. Discussion

In this study, we provide novel information on the tumor microenvironment in primary intestinal tumors and in metastasis of such tumors in Atlantic salmon broodfish. We used material collected after an epizootic incidence of cancer development following chronic, feed-induced enteritis related to the use of plant feed for the carnivorous salmon. In the first report describing the pathological development of adenocarcinoma in salmon, several highly desirable traits for a cancer model were revealed, including feed-induced enteritis, dysplasia, tumorigenesis and metastasis (Dale et al., 2009). Here, we add to the

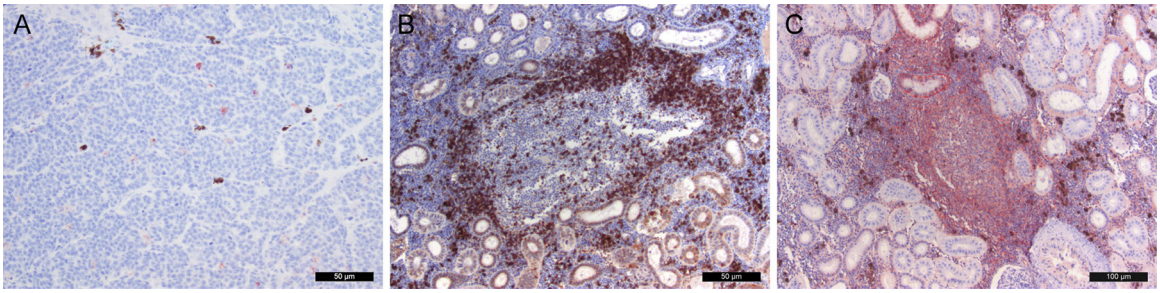

Fig. 7. IHC Immune cells in kidney metastases. A) MHC class II staining showing few MHC class II^+ cells (red) in stroma and cancer islets. Note the presence of melano-macrophages in the stroma. B) CD3 staining showing aggregation of T cells (brown) surrounding tumor tissue. C) MHC class I staining of parallel section of B reveals high density of MHC class I^+ cells (red) in this area. Note the presence of melano-macrophages in the surrounding stroma and interstitial tissue.

previous description of the condition, by describing the stroma and showing the distribution of different immune cells in both primary tumors and in metastases.

In all intestinal tumors, we identified a prominent and well-developed stroma. The amount of stroma in the metastases varied, but was most developed in the hepatic metastases, where a pronounced desmoplastic reaction was observed in one individual. It has previously been assumed that the stroma provides protection against invading cancer cells (Hewitt et al., 1993), however, more recent studies of colorectal cancer in humans have shown the opposite; that the stroma actually can support tumor progression (Kalluri and Zeisberg, 2006, Cirri and Chiarugi, 2011, Sund and Kalluri, 2009, Radisky et al., 2002). This corresponds well with the fact that all primary tumors in the present study had a pronounced stroma and were associated with numerous metastases. Thus, the evidence for stromal promotion of tumor cells in humans might also apply in salmon adenocarcinoma. Interestingly, the heart metastases were totally devoid of any supporting stroma. During the epizootic incident Dale et al., 2009, heart metastases were only found by histology and no large, macroscopic tumors were observed in hearts. Cardiac metastases of intestinal adenocarcinomas are rare in humans and detailed descriptions of possible tumor stroma were not available for comparison between salmon and other species (Patel et al., 2012).

Mast cells were identified by MSB staining. Judging by numbers alone, mast cells seem to play a larger role in the primary tumors than in the metastases. This could be related to the amount of stroma in primary tumors versus metastases as mast cells were mainly observed in the stroma. Another aspect is that these cells are normally present in large numbers in the intestinal mucosa of many fish species, but less prominent in other organs (Hellberg et al., 2013; Reite and Evensen, 2006). Few mast cells were present in the intestinal epithelium in tumors, this being in contrast to observations in mammals (Khazaie et al., 2011). Mast cell degranulation was more prominent at the edges of tumor tissue and in the inflamed mucosa, consistent with their participation in the promotion of chronic inflammation. This is in accordance with observations in mammals (Theoharides and Conti, 2004). Mast cells in mammals and teleosts contain proteases that degrade the extracellular matrix (Khazaie et al., 2011; Baccari et al., 2011), and therefore, the mast cells could play a role in the destruction of the *stratum compactum* and thereby promote tumor invasion in the intestinal wall of Atlantic salmon and further metastasis. Mast cells did not label positive for MHC class II that is consistent with earlier work on MHC class II in salmonids (Koppang et al., 2003). Mammalian mast cells do not usually express MHC class II, but expression can be induced *in vitro* (Kambayashi et al., 2009).

Both mast cells and T cells were more numerous at the invasive front of the tumors than the luminal front. In a mouse model, a T cell-dependent mast cell response appears to promote small bowel cancer (Saadalla et al., 2018). The co-variance of mast cell and T cell distribution in the present material may indicate a similar relationship in teleosts.

Large numbers of $CD3^+$ cells were identified by IHC in primary tumors with a similar distribution to that observed in human colorectal tumors (Gajewski et al., 2013). Dense foci of $CD3^+$ cells were detected in the stroma, mainly at the invasive front. In the cancerous cell islands, few T cells were observed, usually only as single cells. These findings could suggest that the T cells possess a protective role, as proposed for colorectal cancer in humans (Pages et al., 2005; Laghi et al., 2009).

Fewer T cells were detected in metastases, but the occurrence varied between organs. In the liver, which had most metastases, probably due to direct hematogenous spread of cancer cells from the intestinal primary tumors, few $CD3^+$ cells were present and mainly located to the cancerous cell islets. In addition, scattered $CD3^+$ cells were consistently detected in the adjacent, unaffected liver tissue according to the normal distribution pattern of such cells (Koppang et al., 2010). In cardiac metastases, $CD3^+$ cells did not appear to have an association to tumor tissue. In kidneys, $CD3^+$ cells were present in large numbers, including in tumor tissue.

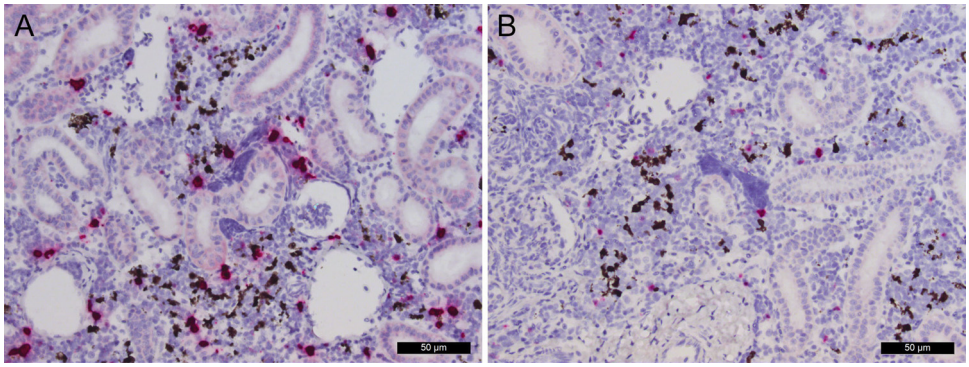

Fig. 8. ISH of kidney metastases targeting IgM and IgT transcripts. A) IgM^+ cells (red) are evenly distributed throughout the interstitial tissue. B). IgT^+ cells (red) show a similar distribution as IgM^+ cells but are present in lower numbers.

In primary tumors, few $CD8^+$, i.e. cytotoxic T cells, were detected and were mainly located within islands of cancerous cells. $CD8^+$ cells were only detected in one liver metastasis confined to a focal area in the tumor tissue. A healthy cytotoxic T cell response in human colorectal cancer is associated with lower metastatic activity and increased survival (Gajewski et al., 2013; Pages et al., 2005; Galon et al., 2006). During the epizootic incident the cancer progressed markedly with respect to prevalence and size of the tumour. In keeping with this, the present results with extensive metastatic activity may indicate that a poor $CD8^+$ cell response is deleterious also in teleost fish. This could reflect a failing immune response in Atlantic salmon brood fish, which seldom survive spawning in their natural environment.

In the present study, macrophage-like cells were not abundant in the intestinal tumor stroma, neither on the luminal side nor on the invasive front of tumors, as MHC class II^+ cells were mainly confined to the clusters of cancerous cells. This is in accordance with observations in human colon cancer, where a high density of tumor-associated macrophages (TAM) at the invasive front is inversely correlated to hepatic metastasis (Zhou et al., 2010). However, MHC class II^+ cells were present in higher numbers in inflammatory lesions and surrounding ectopic epithelium, i.e. the early stages of the enteritis – dysplasia – tumorigenesis pathway (Dale et al., 2009; Bjørgen et al., 2018).

In the intestine, high numbers of IgM^+ cells were observed in inflamed and intact *lamina propria* and on the luminal front of tumors. IgT^+ cells showed a similar distribution, but in lower numbers. This is in contrast to the situation in healthy salmon, where IgM^+ cells are present in small numbers in the intestinal *lamina propria* and transcript levels of IgT in intestine are not conspicuously high (Løkka et al., 2014). Thus, a B cell response to tumors was seen in our material, similar to the situation in mammals, where a high density of B cells in the tumor microenvironment may impair tumor growth (Germain et al., 2015; Knief et al., 2016). Such a role for the B-cells in the salmon was not evident, and possibly, the increase in B cells could be related to their proposed crucial role in the establishment of chronic inflammation leading to carcinogenesis (de Visser et al., 2005).

In metastases, the distribution of IgM^+ and IgT^+ cells varied somewhat between organs and a clear B cell response could not be observed in cardiac and kidney tumors. In the liver, IgM^+ cells were mostly detected peri- and intravascularly in the parenchyma and at the tumor-host interface. IgM^+ and IgT^+ cells were also detected among cancerous cells and in the stroma. In human colorectal cancer, the number of B cells is lower in hepatic metastases than in primary tumors (Shimabukuro-Vornhagen et al., 2014). In addition, B cells in primary tumors are mainly terminally differentiated memory B cells or plasma cells while metastases are dominated by regulatory B cells, suggesting that the specific immune response is more prominent against primary tumors than metastases.

The occurrence and distribution of immune cells varied between primary tumors and metastases, the main difference being a higher density of mast cells, T cells and IgM^+ cells in the primary intestinal tumors versus liver, kidney and heart metastases. In addition, there were differences between metastatic organs with $CD3^+$ cells being present in kidney in much higher numbers than liver or heart. The observed differences between primary tumors and metastases may in part be due to variations in normal cell populations in the different organs, such as the large numbers of mast cells in the salmonid intestine compared to other tissues or the fact that the kidney is a lymphoid organ where $CD3^+$ cells are present throughout the interstitial tissue (Koppang et al., 2010). Another aspect is that the high numbers of mast cells, T cells and B cells in primary tumors vs. metastases reflects the chronic inflammation that is present in the intestine but not the metastatic organs. These cells are key players in the initiation and maintenance of carcinogenic chronic inflammation in higher vertebrates (Theoharides and Conti, 2004; de Visser et al., 2005; Monteleone et al., 2012).

To conclude, we have presented the first investigation of the tumor microenvironment and stroma in fish. The case of adenocarcinoma in Atlantic salmon brood fish is intriguing as it has the capacity to metastasize, which is highly desirable in an animal model. We have shown that the tumors share many of the immunological features of colorectal cancer in humans. The cellular reactions and host responses thus seem phylogenetically well conserved between fish and mammals with respect to the inflammation-dysplasia-carcinogenesis pathway in the development of intestinal adenocarcinoma.

Acknowledgements

We thank VMD Brit Tørud (Norwegian Veterinary Institute) for collecting tissues when performing health surveillance of brood stock. Prof. Ivar Hordvik (University of Bergen) is thanked for providing the sequences used in the probe design for ISH studies. Ms. C. Linde (Department of Basic Sciences and Aquatic Medicine, NMBU, Faculty of Veterinary Medicine, Norway) is acknowledged for laboratory assistance. Dr. Karsten Skjødt (Department of Cancer and Inflammation Research, SDU, Denmark) is acknowledged for providing antibodies.

References

Baccari, G.C., Pinelli, C., Santillo, A., Minucci, S., Rastogi, R.K., 2011. Mast cells in nonmammalian vertebrates: an overview. Int. Rev. Cell Mol. Biol. 290, 1–53.
Bancroft, J.D., Gamble, M., 2008. Theory and Practice of Histological Techniques. Elsevier Health Sciences.
Bjørgen, H., Koppang, E.O., Gunnes, G., Hordvik, I., Moldal, T., Kaldhusdal, M., et al., 2018. Ectopic epithelial cell clusters in salmonid intestine are associated with inflammation. J. Fish Dis.
Burns, A.R., Watral, V., Sichel, S., Spagnoli, S., Banse, A.V., Mittge, E., et al., 2018. Transmission of a common intestinal neoplasm in zebrafish by cohabitation. J. Fish Dis. 41, 569–579.
Cirri, P., Chiarugi, P., 2011. Cancer associated fibroblasts: the dark side of the coin. Am. J. Cancer Res. 1, 482.
Dale, O.B., Tørud, B., Kvellestad, A., Koppang, H.S., Koppang, E.O., 2009. From chronic feed-induced intestinal inflammation to adenocarcinoma with metastases in salmonid fish. Cancer Res. 69, 4355–4362.
de Visser, K.E., Korets, L.V., Coussens, L.M., 2005. De novo carcinogenesis promoted by chronic inflammation is B lymphocyte dependent. Cancer Cell 7, 411–423.
Etchin, J., Kanki, J.P., Look, A.T., 2011. Zebrafish as a model for the study of human cancer. Methods Cell Biol. 105, 309–337.
Gajewski, T.F., Schreiber, H., Fu, Y.X., 2013. Innate and adaptive immune cells in the tumor microenvironment. Nat. Immunol. 14, 1014–1022.
Galon, J., Costes, A., Sanchez-Cabo, F., Kirilovsky, A., Mlecnik, B., Lagorce-Pages, C., et al., 2006. Type, density, and location of immune cells within human colorectal tumors predict clinical outcome. Science (New York, NY) 313, 1960–1964.
Germain, C., Gnjatic, S., Dieu-Nosjean, M.C., 2015. Tertiary lymphoid structure-associated B cells are key players in anti-tumor immunity. Front. Immunol. 6, 67.
Giraldo, N.A., Sanchez-Salas, R., Peske, J.D., Vano, Y., Becht, E., Petitprez, F., et al., 2019. The clinical role of the TME in solid cancer. Br. J. Cancer 120, 45–53.
Hellberg, H., Bjerkås, I., 2000. The anatomy of the oesophagus, stomach and intestine in common wolffish (*Anarhichas* lupus L.): a basis for diagnostic work and research. Acta Vet. Scand. 41, 283–298.
Hellberg, H., Bjerkås, I., Vagnes, O.B., Noga, E.J., 2013. Mast cells in common wolffish Anarhichas lupus L.: ontogeny, distribution and association with lymphatic vessels. Fish Shellfish Immunol. 35, 1769–1778.
Hewitt, R.E., Powe, D.G., Ian Carter, G., Turner, D.R., 1993. Desmoplasia and its relevance to colorectal tumour invasion. Int. J. Cancer 53, 62–69.
Kalluri, R., Zeisberg, M., 2006. Fibroblasts in cancer. Nat. Rev. Cancer 6, 392.
Kambayashi, T., Allenspach, E.J., Chang, J.T., Zou, T., Shoag, J.E., Reiner, S.L., et al., 2009. Inducible MHC class II expression by mast cells supports effector and regulatory T cell activation. J. Immunol. (Baltimore, Md: 1950) 182, 4686–4695.
Khazaie, K., Blatner, N.R., Khan, M.W., Gounari, F., Gounaris, E., Dennis, K., et al., 2011. The significant role of mast cells in cancer. Cancer Metastasis Rev. 30, 45–60.
Knief, J., Reddemann, K., Petrova, E., Herhahn, T., Wellner, U., Thorns, C., 2016. High Density of Tumor-infiltrating B-Lymphocytes and Plasma Cells Signifies Prolonged Overall Survival in Adenocarcinoma of the Esophagogastric Junction. Anticancer Res. 36, 5339–5345.
Koppang, E.O., Hordvik, I., Bjerkas, I., Torvund, J., Aune, L., Thevarajan, J., et al., 2003. Production of rabbit antisera against recombinant MHC class II beta chain and identification of immunoreactive cells in Atlantic salmon (*Salmo salar*). Fish Shellfish Immunol. 14, 115–132.
Koppang, E.O., Fischer, U., Moore, L., Tranulis, M.A., Dijkstra, J.M., Köllner, B., et al., 2010. Salmonid T cells assemble in the thymus, spleen and in novel interbranchial lymphoid tissue. J. Anat. 217, 728–739.
Laghi, L., Bianchi, P., Miranda, E., Balladore, E., Pacetti, V., Grizzi, F., et al., 2009. CD3+ cells at the invasive margin of deeply invading (pT3-T4) colorectal cancer and risk of post-surgical metastasis: a longitudinal study. Lancet Oncol. 10, 877–884.
Liu, S., Leach, S.D., 2011. Zebrafish models for cancer. Annu. Rev. Pathol. 6, 71–93.

Løkka, G., Austbø, L., Falk, K., Bjerkås, I., Koppang, E.O., 2013. Intestinal morphology of the wild Atlantic salmon (*Salmo salar*). J. Morphol. 274, 859–876.
Løkka, G., Austbø, L., Falk, K., Bromage, E., Fjelldal, P.G., Hansen, T., et al., 2014. Immune parameters in the intestine of wild and reared unvaccinated and vaccinated Atlantic salmon (*Salmo salar* L.). Dev. Comp. Immunol. 47, 6–16.
Lyngstad, T.M., Brun, E., Norstrøm, M., Eriksen, G.S., Dale, O.B., Lillehaug, A., 2007. Tarmsvulst hos stamfisk laks—epidemiologisk undersøkelse. Norwegian Veterinary Institute report.
Monteleone, G., Pallone, F., Stolfi, C., 2012. The dual role of inflammation in colon carcinogenesis. Int. J. Mol. Sci. 13, 11071–11084.
Pages, F., Berger, A., Camus, M., Sanchez-Cabo, F., Costes, A., Molidor, R., et al., 2005. Effector memory T cells, early metastasis, and survival in colorectal cancer. N. Engl. J. Med. 353, 2654–2666.
Patel, S.A., Herfel, B.M., Nolan, M.A., 2012. Metastatic colon cancer involving the right atrium. Tex. Heart Inst. J. 39, 79–83.
Paquette, C.E., Kent, M.L., Buchner, C., Tanguay, R.L., Guillemin, K., Mason, T.J., et al., 2013. A retrospective study of the prevalence and classification of intestinal neoplasia in zebrafish (Danio rerio). Zebrafish 10, 228–236.
Radisky, D., Muschler, J., Bissell, M.J., 2002. Order and disorder: the role of extracellular matrix in epithelial cancer. Cancer Invest. 20, 139–153.
Reite, O.B., Evensen, O., 2006. Inflammatory cells of teleostean fish: a review focusing on mast cells/eosinophilic granule cells and rodlet cells. Fish Shellfish Immunol. 20, 192–208.
Saadalla, A.M., Osman, A., Gurish, M.F., Dennis, K.L., Blatner, N.R., Pezeshki, A., et al., 2018. Mast cells promote small bowel cancer in a tumor stage-specific and cytokine-dependent manner. Proc. Natl. Acad. Sci. U. S. A. 115, 1588–1592.
Shimabukuro-Vornhagen, A., Schlosser, H.A., Gryschok, L., Malcher, J., Wennhold, K., Garcia-Marquez, M., et al., 2014. Characterization of tumor-associated B-cell subsets in patients with colorectal cancer. Oncotarget 5, 4651–4664.
Sund, M., Kalluri, R., 2009. Tumor stroma derived biomarkers in cancer. Cancer Metastasis Rev. 28, 177–183.
Theoharides, T.C., Conti, P., 2004. Mast cells: the Jekyll and Hyde of tumor growth. Trends Immunol. 25, 235–241.
Vergneau-Grosset, C., Nadeau, M.E., Groff, J.M., 2017. Fish oncology: diseases, diagnostics, and therapeutics. Vet. Clin. North Am. Exot. Anim. Pract. 20, 21–56.
Yasuike, M., De Boer, J., von Schalburg, K.R., Cooper, G.A., McKinnel, L., Messmer, A., et al., 2010. Evolution of duplicated IgH loci in Atlantic salmon, Salmo salar. BMC Genomics 11, 486.
Yee, N.S., Ignatenko, N., Finnberg, N., Lee, N., Stairs, D., 2015. Animal models of cancer biology. Cancer Growth Metastasis 8, 115–118.
Zhou, Q., Peng, R.Q., Wu, X.J., Xia, Q., Hou, J.H., Ding, Y., et al., 2010. The density of macrophages in the invasive front is inversely correlated to liver metastasis in colon cancer. J. Transl. Med. 8, 13.